Journal of Materials Chemistry B

ROYAL SOCIETY OF CHEMISTRY

PAPER

View Article Online
View Journal | View Issue

Cite this: J. Mater. Chem. B, 2022, 10, 6958

Orientation-controlled crystallization of γ-glycine films with enhanced piezoelectricity†

Jiajie Sui,[a] Jun Li,[a] Long Gu,[a] Connor A. Schmidt,[b] Ziyi Zhang,[a] Yan Shao,[a] Ehud Gazit,[c] Pupa U. P. A. Gilbert‡[bde] and Xudong Wang *[a]

Received 7th May 2022,
Accepted 10th August 2022

DOI: 10.1039/d2tb00997h

rsc.li/materials-b

Glycine, the simplest amino acid, is considered a promising functional biomaterial owing to its excellent biocompatibility and strong out-of-plane piezoelectricity. Practical applications require glycine films to be manufactured with their strong piezoelectric polar ⟨001⟩ direction aligned with the film thickness. Based on the recently-developed solidification approach of a polyvinyl alcohol (PVA) and glycine aqueous solution, in this work, we demonstrate that the crystal orientation of the as-synthesized film is determined by the orientation of glycine crystal nuclei. By controlling the local nucleation kinetics *via* surface curvature tuning, we shifted the nucleation site from the edge to the middle of the liquid film, and thereby aligned the ⟨001⟩ direction vertically. As a result, the PVA–glycine–PVA sandwich film exhibits the highest aver-age piezoelectric coefficient d_{33} of 6.13 ± 1.13 pC N^{-1}. This work demonstrates a promising kinetic approach to achieve crystallization and property control in a scalable biocrystal manufacturing process.

Introduction

Piezoelectric materials that couple mechanical and electric energy have demonstrated great potential in biomedical applications.[1] Currently, they have already been widely used in wearable and implantable energy-harvesting devices,[2,3] motion sensors[4,5] and scaffolds for tissue-engineering.[6] Limitations of conventional piezoelectric materials encouraged the emergence of novel biological piezoelectric materials with high flexibility, desired biocompatibility and biodegradability.[7,8] Amino acids, a fundamental building block of the human body and one of the simplest biomaterials, are recently re-emerged as a promising piezoelectric biomaterial[7,9,10] with theoretical piezoelectric coefficients comparable to conventional piezoelectric soft materials such as polyvinylidene difluoride (PVDF)[11] and zinc oxide.[12] In addition, most types of amino acids are piezoelectric due to their non-centrosymmetric crystal structures.[13]

Glycine is the simplest and most studied amino acid, which has three different polymorphs, *i.e.* α-, β- and γ-glycine.[14–16] α-Glycine does not exhibit any bulk piezoelectricity due to the elimination of dipole in the crystal. β-Glycine is predicted to show outstanding shear piezoelectricity (d_{16} ∼ 178 pC N^{-1}),[17] but is meta-stable and can easily transform into the other two phases in atmosphere. γ-Glycine is stable and has a theoretical longitudinal piezoelectric coefficient, d_{33} up to 10.4 pC N^{-1} (along the ⟨001⟩ direction),[18] and is considered the most promising phase. However, reported experimental piezoelectricity is much lower than the theoretical value due to the randomness of the crystal domain orientations. Studies suggested that interfacial interactions such as hydrogen bonding or van der Waals force may guide the direction of crystal growth.[17,19] A most recent report revealed that the rich hydrogen bonds at the glycine and polyvinyl alcohol (PVA) interface could align all the interface-nucleated γ-glycine crystals along the same direction, and thus boosted the bulk piezoelectricity d_{33} up to 5.3 pC N^{-1}.[20] Nonetheless, this value was still only half of the theoretical value, mostly because the polarization ⟨001⟩ direction was not perpendicular to the film surface. This non-preferred crystal orientation was a result of the nuclei (001) facets being aligned with the tilted edge of the liquid precursor film, where the convex liquid surface makes it the most energy favorable region for nucleation. It is therefore intuitive to hypothesize that if the nuclei (001) facets can be tuned horizontally, the bulk piezoelectricity of the film may be further enhanced. In this paper, we present that by tuning the

[a] Department of Materials Science and Engineering, University of Wisconsin, Madison, WI 53706, USA. E-mail: xudong.wang@wisc.edu
[b] Department of Physics, University of Wisconsin, Madison, WI 53706, USA
[c] Shmunis School of Biomedicine and Cancer Research, George S. Wise Faculty of Life Sciences, and Department of Materials Science and Engineering, The Iby and Aladar Fleischman Faculty of Engineering, Tel Aviv University, Tel Aviv, Israel
[d] Departments of Chemistry, Materials Science and Engineering, Geoscience, University of Wisconsin, Madison, WI 53706, USA
[e] Chemical Sciences Division, Lawrence Berkeley National Laboratory, Berkeley, CA 94720, USA

† Electronic supplementary information (ESI) available. See DOI: https://doi.org/10.1039/d2tb00997h

‡ Previously publishing as Gelsomina De Stasio.

liquid film contact angle, the nuclei crystal orientation could be adjusted accordingly. Guided by this discovery, the liquid film edge was tuned from convex to concave, and thereby successfully moved the preferred nucleation sites to the center of the film, where the heterogeneous water–PVA interface guided the (001) glycine facets parallel to the film surface. Tuning the crystal orientation of the glycine film enhanced the film's bulk d_{33} and their piezoelectric output. This work demonstrated a promising example of using interfacial energy to tune the nucleation and thus control the bulk film's piezoelectric property, which may serve as a facile engineering tool for advanced biocrystal manufacturing.

Results and discussion

It was recently discovered that the hydrogen bonds between the hydroxyl (–OH) group of PVA and the carboxyl (–COOH) group of glycine are the most energy-favorable interaction (calculated binding energy of up to 1 eV).[20] Therefore, when a PVA surface is present, glycine nuclei would preferably align their (001) facets parallel to the chain of PVA molecules at the interface (Fig. 1a), and thus the strongest piezoelectric polarization ⟨001⟩ direction of glycine is perpendicular to the PVA–glycine interface at the nucleation sites. The PVA–glycine interface could be formed automatically and continuously by the solidification of a glycine/PVA mixture solution. PVA would precipitate out first due to its lower water solubility and the salting out effect,[21] and accumulate at the top and bottom of the aqueous solution due to the surface tension.[22,23] Glycine started nucleation with subsequent water evaporation and these nuclei led to continuous and coherent glycine crystal growth, forming a PVA–glycine–PVA sandwiched structure with all glycine crystal domains aligned in the same direction. From a typical aqueous film configuration that is needed to grow a large glycine film, glycine initially nucleates near the edge under the convex top surface,[24] where a high supersaturation and high interface free energy exist (Fig. 1b).[25] Therefore, the (001) plane of glycine crystal would incline against the horizontal substrate plane at a certain angle (θ). This inclination angle would persist across the entire film due to the coherent growth of glycine crystals as the aqueous film dries. Therefore, the strongest piezoelectric polarization of γ-glycine is roughly shifted θ away from the film's normal direction, so that the effective 33 direction piezoelectric response is jeopardized.

Fig. 1b also suggests that the angle θ is dependent on the curvature of top liquid surface, and thus could be controlled by the liquid-substrate contact angle. To investigate the effect of contact angles on crystal directions, glycine–PVA films were synthesized on three substrates with different contact angles (insets of Fig. 1c): polymethyl methacrylate (PMMA) 54.3°, polystyrene (PS) 65.4° and polydimethylsiloxane (PDMS) 92.1°. All the three systems yielded a continuous wafer-scale film with a clear PVA–glycine–PVA sandwiched structure (Fig. 1c). All the films were nucleated along the edge and grow toward the center. The thickness of each film was in the range of 30–40 μm (Fig. S1, ESI†). As the low energy (001) planes are typically the cleavage surface, the line features in the cross-sectional scanning electron microscopy (SEM) indicates the position of the (001) facets. Therefore, the angle α between ⟨001⟩ polarization direction and normal direction of film were measured to be: 54.7°, 34.1° and 57.8°, for PMMA, PS and PDMS, respectively. X-ray powder diffraction spectra (Fig. 1d) of the three samples exhibited similar peak distributions, revealing that the glycine crystals were all γ phase. The relatively stronger (102) peaks from the PMMA- and PS-supported films also indicate a better alignment of the polar directions of all glycine crystals. Based on the crystal structure of γ-glycine,[16] the facet arrangement of (001), (110) and (101) is shown in Fig. 1e, where the horizontal and normal directions to the film plane were represented by *x*- and *y*-axis, respectively. From this geometric relationship, the direction of the (001) facets can be determined from the orientation of the (110) facet, because that the (001) peak does not show in the XRD spectra. As thus, the piezoelectric polarization ⟨001⟩ direction was tilted 54.7°, 34.1° and 57.8° from the normal direction for films grown on PMMA, PS and PDMS substrates, respectively. The non-linear relationship between θ and the wetting angle would possibly be the change of the wetting situation during the water evaporation process.[26] The out-of-plane piezoelectricity, d_{33}, which is directly related to the fractional vector of the ⟨001⟩ direction on the normal direction, was found to be 4.24 pC N^{-1}, the highest for the glycine films grown on PS substrates (Table S1, ESI†). The d_{33} dropped to 3.44 and 1.56 pC N^{-1} for glycine films on PMMA and PDMS substrates, respectively, in accordance with their larger contact angles. The lower piezoelectric performance of PDMS-supported glycine film could be attributed to the relatively larger amount of misoriented glycine crystals in the film (Fig. 1e). This result clearly proved that tuning the polarized (001) facet toward the film surface is effective in improving the film's bulk d_{33}.

The substrate-dependent growth study revealed that the out-of-plane piezoelectricity, d_{33} of the glycine–PVA films was largely determined by the initial nucleation orientation, which controls the orientation of the glycine ⟨001⟩ direction thereafter. Therefore, we hypothesize that the best orientation alignment may be achieved if the nucleation site moves to the flat liquid surface in the middle area. Gibbs-Thompson relationship[27] suggests that surfaces with a negative surface curvature (K) have a lower equilibrium vapor pressure than that at flat surfaces, and could lower the local evaporation rate thus to slow down the supersaturation building up. Experimentally, the negative K at the liquid edge was achieved by attaching a glass wall around the glycine–PVA liquid film on a PS substrate (PS + wall) (Fig. 2a). Thus, water evaporation was lowered around the liquid film edges, and thereby the supersaturation under the flat solution surface became higher than the edge region.[24] Together with the lower surface tension,[25] nucleation would become more thermodynamically and kinetically favorable at the middle flat area (Fig. 2b).

The optical image of as-grown films (Fig. 2c) clearly shows that the nucleation site moved away from the edge to the lower middle area. Areas around the nucleation site showed clear

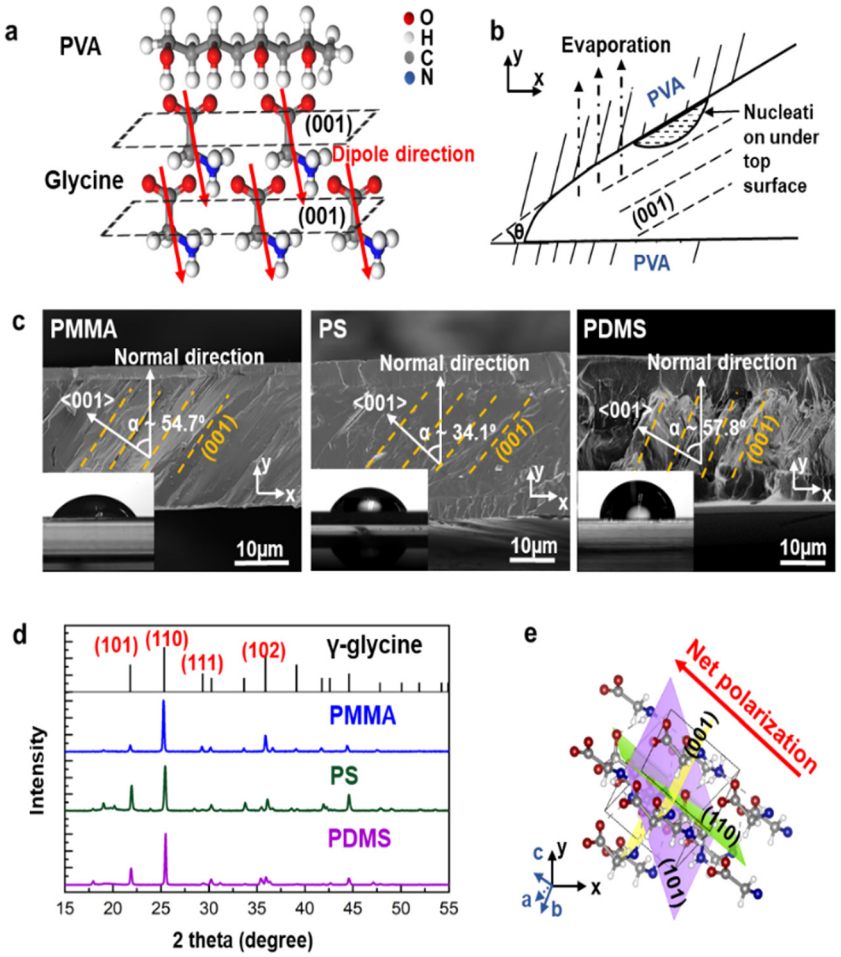

Fig. 1 PVA–glycine films grown on different substrates. (a) Schematic of the hydrogen binding between glycine molecules and PVA chains. (b) Schematic illustration of the initial nucleation sites at the curved edge of the liquid film. (c) Cross-sectional SEM imag-es of PVA–glycine films on PMMA, PS and PDMS substrates. Insets are corresponding contacting angle test. (d) XRD spectra of glycine–PVA films on PMMA (blue), PS (green) and PDMS (purple) substrates. (e) Schematic crystal structure of glycine crystal revealing the arrangement of (001), (101) and (110) planes.

radial crystal feature indicating the crystal growth directions. Crystals exhibited vertically aligned features both inside and outside the nucleation region, while the nucleation region had an incomplete coverage of glycine crystals and small crystal sizes (Fig. S2, ESI†). Cross-sectional SEM and EDS mapping of nitrogen (N) element (Fig. 2d) revealed that the film still preserved the three-layer sandwiched structure with a total thickness of 28 μm, and the glycine middle layer of 16 μm. The grains of glycine crystals exhibited similar elongated shape along their growth direction, with a width of 100 μm and up to 2 mm in length (Fig. S3, ESI†). XRD spectra (Fig. 2e) of the PS + wall samples showed a substantially enhanced (102) peak and almost diminished (110) peak compared to the films grown without wall, indicating that the (102) facets were more parallel to the film plane while the (110) facets were perpendicular to the film surface. Fig. 2f reveals the arrangement of (001), (102) and (110) facets in a γ-glycine crystal. The (102) and (001) facets are only 24.2° from each other, and the (110) and (001) facets are normal to each other. Therefore, although the (001) peak cannot show in XRD spectra, the very strong (102) peak and nearly diminished (110) peak evidenced the (001) plane of glycine was mostly parallel to the film surface. This is the preferred orientation to enhance the out-of-plane piezoelectricity.

The glycine–PVA film growth behavior on PS surface with and without walls was recorded and compared to shed light on the film crystallization kinetics. The fractions of the crystalized area were quantified as a function of time and fitted into the Johnson–Mehl–Avarami–Kolmogorov (JMAK) relation[28,29] using the following equation:

$$X(t) = 1 - \exp[-(kt)^n]$$

where $X(t)$ is area transition fraction, k is rate constant, t is time and n is morphology index. In our case, $X(t)$ was determined from the ratio of crystalline area to overall film size. Well-fitted curves of growth process were achieved by assuming $n = 2$, suggesting the growth could be considered as two-dimensional. As shown in Fig. 3, when the wall was introduced, the glycine–PVA films took almost twice the time to nucleate as that on flat PS surfaces. This could be attributed to the higher nucleation barrier and slower evaporation rate at the flat area compared to

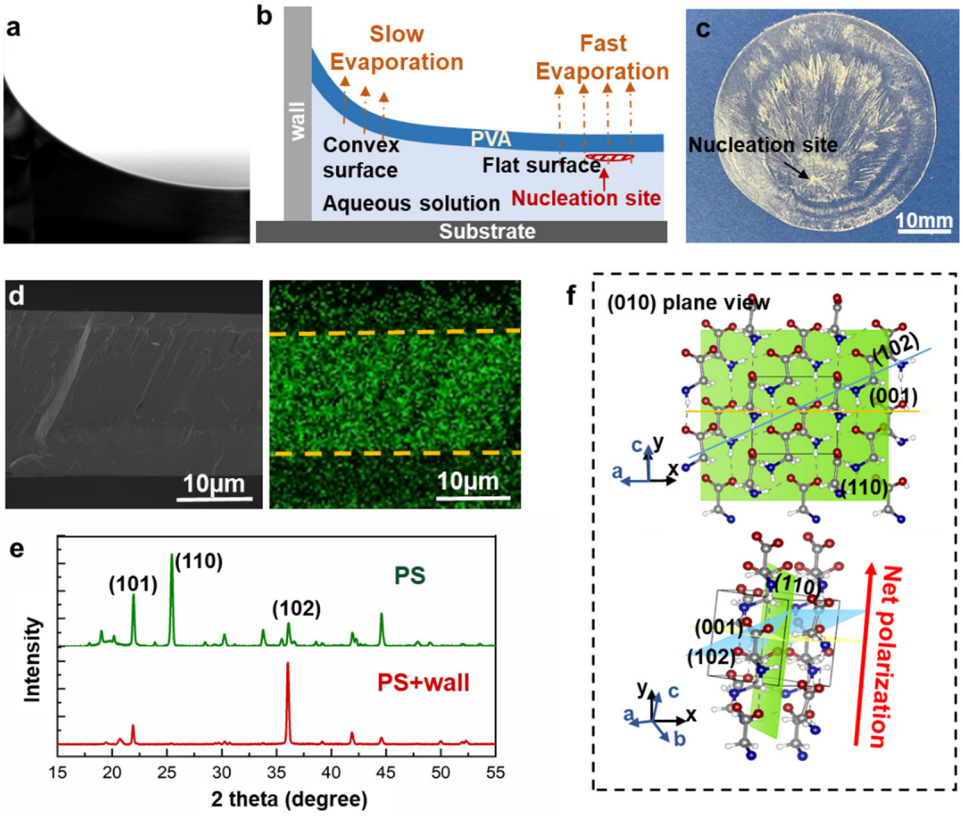

Fig. 2 Growth of PVA–glycine films with a normal ⟨001⟩ orientation. (a) Optical image showing the concaved solution surface along the edge when a vertical wall was applied. (b) Schematic illustration of nucleation site at the center flat area of the film. (c) Digital photograph of an as-grown film showing the nucleation spot and wafer scale size. (d) Cross-sectional SEM image (left) and corre-sponding EDS map of N (right) confirming the same PVA–glycine–PVA sandwiched structure. (e) XRD spectra of films grown on PS (green) and PS plus wall (red) substrates confirming the switching of film crystal orientation. (f) Schematic glycine crystal structure showing the direction relationship of (001) and (102).

the convex edge with a positive surface curvature. The growth process of the glycine–PVA films on PS + wall substrates could be fitted to two stages: rapid growth at the beginning and decreased growth rate when approaching the edge. Rate constants (k) were calculated to be 1.71×10^{-6} for the first stage, close to the films grown without wall ($k = 2.62 \times 10^{-6}$). The close k values further testified their similar energy barrier as both glycine crystal growth occurred under a flat liquid surface and driven by similar water evaporation rates. Decreased growth rate at the second stage as the crystal approaching edges could be attributed to the consumption of glycine precursor along the expanding growth front together with the decreased water evaporation rate under negative surface curvatures.

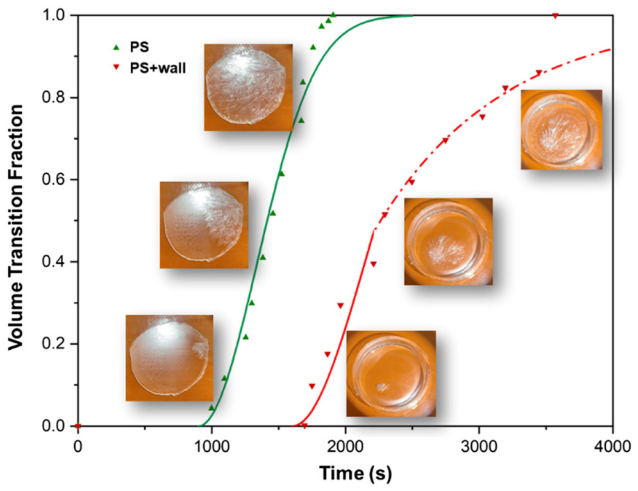

Fig. 3 Kinetics of glycine–PVA films growth on PS surface with (green) and without walls (red). Each dot represents the ratio between crystalline area to the overall film area from an optical image (insets) taken during the film growth process. The smooth lines are fitted curves based on the JMAK theory.

It is expected that tuning the crystal orientation to the (001) facet would better tune the piezoelectric polarization to the normal direction and thus improve the out-of-plane piezoelectricity. To evidence the preferably aligned piezoelectric polarization, second harmonic generation (SHG) was conducted on exposed glycine top surface and compared to films grown without walls (Fig. 4a). The (001)-oriented glycine film exhibited strong and uniform polarization intensity, indicating the polarization domain was mostly aligned along the normal direction. In contrast, the surface of glycine film grown without wall showed much less and non-uniform contrast. The out-of-plane piezoelectric coefficient, d_{33} was measured to be 6.13 ± 1.13 pC N^{-1} over the full-coverage area outside the nucleation region (Fig. S4, ESI†) with a maximum of 8.0 pC N^{-1}. It was a significant increase as compared to the films

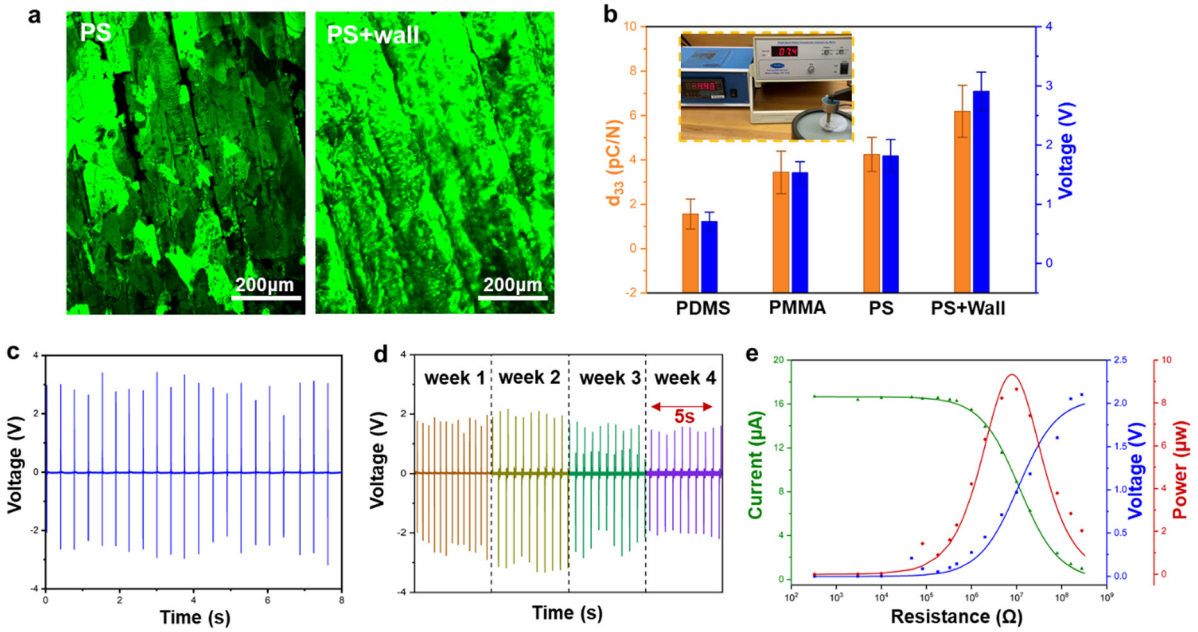

Fig. 4 Piezoelectric properties of the (001)-oriented glycine–PVA films. (a) SHG images of the glycine surface from the (001)-oriented glycine–PVA films (PS + wall) and mis-oriented glycine–PVA film (PS). (b) Comparison of d_{33} coefficients and piezoelectric voltage output measured of glycine–PVA films grown on different substrates with different crystal orientations. (c) Piezoelectric voltage output of the (001)-oriented glycine–PVA film measured under a 30-N impulse force. (d) Long-term time-dependent piezoelectric outputs. (e) Load-resistance curve of the (001)-oriented glycine–PVA film.

grown without using walls on various substrates (Fig. 4b and Fig. S5, ESI†). This measurement further confirmed the significance of aligning the ⟨001⟩ direction for the improvement of out-of-plane piezoelectricity.

To demonstrate the application potential as a mechanical energy harvester, the out-of-plane piezoelectric voltage output was measured from the (001)-oriented glycine–PVA films by coating both surfaces with a 1 cm^2 copper electrodes. Compared to the other films (Fig. S6 and Table S1, ESI†), under 30 N impulse forces at 3 Hz, the glycine–PVA films generated a stable piezoelectric voltage output with an average of 2.9 V and highest peak-to-peak voltage of 6.1 V (Fig. 4c), and a consistent current output of 16 μA (Fig. S7, ESI†). Subsequent voltage measurements were taken under the same conditions for 4 weeks. The film showed nearly constant voltage outputs within the range from 2.0 to 3.0 V (Fig. 4d), suggesting the long-term stable piezoelectricity in atmosphere. γ-Glycine crystals covered by double PVA layers was able to preserve the crystallinity and piezoelectric performance for over two weeks in a humid environment (room temperature, 80–90% humidity, Fig. S8, ESI†). To quantify the practical power output capability, output current and voltage were measured across a serious of load resistance from 100 Ω to 10 GΩ. The instantaneous output power was calculated based on the product of peak voltage and current, which revealed the maximum output power of 9.2 μW at a load resistance of 9 MΩ (Fig. 4e).

Experimental

Preparation of substrates

PMMA (100 mm in diameter and 5 mm in thickness) and PS (Petri dish, 100 mm in diameter and 15 mm in height) substrates were ultrasonically cleaned in ethanol once and DI water twice for 20 min. PDMS substrate was fabricated by spin-coating PDMS (10 : 1) at 1000 rpm for 60 s on a glass plate (75 mm × 51 mm). Then the PDMS-coated substrate was moved to 80 °C oven until totally dried. PS + wall substrate was fabricated by physically attaching a glass ring (40 mm in diameter and 10 mm in height) on top of a PS substrate.

Synthesis of glycine–PVA sandwiched films

PVA in water solution (10% w/v) was prepared by dissolving 10 g PVA (Mw 13 000–23 000) in 100 mL deionized water. Glycine solution (10% w/v) was obtained by dissolving 10 g glycine in 100 mL deionized water. 30 mL of 10% glycine solution was added into 10 mL of 10% PVA solution to obtain a glycine–PVA solution with glycine-to-PVA ratio of 3 : 1. A homogeneous solution was obtained by stirring the mixture for 1 h. The as-prepared solution was then directly used for film growth. At room temperature, 1 mL of the mixture solution was slowly applied to different substrates to create a round-shape liquid film with 40 mm diameter. Then the whole system was moved into a convection oven at 60 °C and dried overnight. The as-received glycine–PVA films were directly peeled off by tweezers from the substrates at room temperature in atmosphere for characterizations.[20]

Structure and morphology characterization

SEM observations and EDS characterizations of the cross-section of glycine–PVA composite film were performed on a Zeiss GeminiSEM 450 field-emission microscope. X-Ray diffraction pattern of glycine–PVA composite films were acquired from the Bruker D8 Discovery with Cu K-alpha radiation.

Kinetics process measurement

The optical images and the video of whole film growth process were taken by phone. Then pictures of films were exported at every 30 s at the nucleation stage as the film transition is fast and every 200 s at the crystal growth stage. The transition fractions (X) were calculated from the measured film sizes by Image J:

$$X = A_c/A_0$$

where A_c is the size of crystallized area and A_0 is the size of the whole film.

Electric performance measurement

For measurements of voltage and current output, small pieces (20 mm × 20 mm) were cut from the whole films and covered with cooper tape (50 μm in thickness) at top and bottom as two electrodes. Then the devices were connected through Cu wire for testing. The 30 N mechanical stimuli force was applied to the devices by a computer-controlled actuator (LinMot E1100) at 3 Hz with amplitude of 1 cm. The piezoelectric voltage outputs were recorded by connecting probes of a multimeter (DMM 6500, Keithley, internal resistance 10 Mohm) to the devices. The short-circuit current was measured by a low-noise current preamplifier (Stanford Research Systems, model SR570) connected with LabVIEW system in the computer. Resistance of varied values are connected to the devices, driven by 30 N force at 3 Hz, voltages were measured for the connected resistance and currents were measured for the whole system. Second harmonic generation (SHG) images were taken by Nikon A1R high definition (HD) multiphoton confocal microscope and signals were measured under 1040 nm radiation from built-in lasers. The piezoelectric d_{33} coefficients were measured by a quasi-static piezoelectric constant d_{33} meter (PKD3-2000-F10N, PolyK Technologies, LLC) under forces in range of 3–5 N.

Conclusions

In summary, we demonstrated a self-assembly approach that effectively aligned the piezoelectric polar ⟨001⟩ direction of γ-glycine to the normal direction of the as-grown film surface, and thereby largely improved the out-of-plane piezoelectricity of the bulk film. This alignment was possible because crystal orientation follows those of the nuclei, which is determined by the surface curvature at the nucleation site, which was confirmed by the contact angle-related crystal orientation tuning. By introducing a wall around the liquid precursor film, the surface curvature along the edge was inverted from positive to negative. Changes in surface curvature suppressed the nucleation at the edge area and forced initial nucleation to the middle of the film, where the surface was flat. Therefore, the (001) surface of glycine nuclei became parallel to the film surface, so as the entire film grown thereafter. Tuning the piezoelectric ⟨001⟩ polar direction of γ-glycine crystal to the thickness direction enhanced the out-of-plane bulk piezoelectricity, with an average d_{33} of $\sim 6.13 \pm 1.13$ pC N^{-1}. This value was more than 20% higher than the d_{33} of films nucleated from the edge, where their ⟨001⟩ directions were tilted away from the normal direction. This work demonstrated a promising approach to improving the bulk piezoelectricity of glycine films by nucleation kinetics control. This strategy may inspire crystal orientation control in advanced manufacturing processes of amino acid- or polypeptide-based bio-crystals with enhanced properties.

Author contributions

J. S. and X. W. conceived the idea, initiated the study, and designed the research program. J. S. carried out SEM, EDS and XRD measurement. J. S. and J. L. performed the contact angle measurement, second harmonic generation imaging and d33 measurement. C. S. did the optical polarized imaging and analysis. J. S. and Z. Z. performed the crystal structure analysis and visualization. L. G., J. S. and Y. S. carried out the electrochemical characterizations. J. S. and X. W. wrote the manuscript. All authors reviewed and commented on the manuscript.

Conflicts of interest

There are no conflicts to declare.

Acknowledgements

This research primarily was supported by the U.S. Department of Energy (DOE), Office of Science, Basic Energy Sciences (BES), under Award # DE-SC0020283. J. S. and X. W. thank the support from the Grainger Institute for Engineering.

Notes and references

1 M. S. Vijaya, *Piezoelectric Materials and Devices: Applications in Engineering and Medical Sciences*, CRC Press, 2012.
2 B. Shi, Z. Li and Y. Fan, *Adv. Mater.*, 2018, **30**, 1801511.
3 J. Li, Y. Long, F. Yang and X. Wang, *Curr. Opin. Solid State Mater. Sci.*, 2020, **24**, 100806.
4 M. T. Chorsi, E. J. Curry, H. T. Chorsi, R. Das, J. Baroody, P. K. Purohit, H. Ilies and T. D. Nguyen, *Adv. Mater.*, 2019, **31**, 1802084.
5 C. Dagdeviren, F. Javid, P. Joe, T. V. Erlach, T. Bensel, Z. Wei, S. Saxton, C. Cleveland, L. Booth, S. McDonnel, J. Collins, A. Hayward, R. Langer and G. Traverso, *Nat. Biomed. Eng.*, 2017, **1**, 807–817.
6 J. Jacob, N. More, K. Kalia and G. Kapusetti, *Inflammation Regener.*, 2018, **38**, 2.
7 D. Kim, S. A. Han, J. H. Kim, J.-H. Lee, S.-W. Kim and S.-W. Lee, *Adv. Mater.*, 2020, **32**, 1906989.
8 C. Li, C. Guo, V. Fitzpatrick, A. Ibrahim, M. J. Zwierstra, P. Hanna, A. Lechtig, A. Nazarian, S. J. Lin and D. L. Kaplan, *Nat. Rev. Mater.*, 2020, **5**, 61–81.
9 S. Guerin, S. A. M. Tofail and D. Thompson, *Cryst. Growth Des.*, 2018, **18**, 4844–4848.

10 V. V. Lemanov, S. N. Popov and G. A. Pankova, *Phys. Solid State*, 2011, **53**, 1191–1193.
11 S. Guo, X. Duan, M. Xie, K. C. Aw and Q. Xue, *Micromachines*, 2020, **11**, E1076.
12 I. B. Kobiakov, *Solid State Commun.*, 1980, **35**, 305–310.
13 D. Vasilescu, R. Cornillon and G. Mallet, *Nature*, 1970, **225**, 635.
14 G. Albrecht and R. B. Corey, *J. Am. Chem. Soc.*, 1939, **61**(5), 1087–1103.
15 Y. Iitaka, *Acta Cryst.*, 1960, **13**, 35–45.
16 Y. Iitaka, *Acta Cryst.*, 1961, **14**, 1–10.
17 S. Guerin, A. Stapleton, D. Chovan, R. Mouras, M. Gleeson, C. McKeown, M. R. Noor, C. Silien, F. M. F. Rhen, A. L. Kholkin, N. Liu, T. Soulimane, S. A. M. Tofail and D. Thompson, *Nat. Mater.*, 2018, **17**, 180–186.
18 H. Klapper and T. Hahn, *International Tables for Crystallography*, 2006, ch. 10.2, vol. A, pp. 804–808.
19 J. F. Kang, J. Zaccaro, A. Ulman and A. Myerson, *Langmuir*, 2000, **16**, 3791–3796.
20 F. Yang, J. Li, Y. Long, Z. Zhang, L. Wang, J. Sui, Y. Dong, Y. Wang, R. Taylor, D. Ni, W. Cai, P. Wang, T. Hacker and X. Wang, *Science*, 2021, **373**, 337–342.
21 R. Sadeghi and F. Jahani, *J. Phys. Chem. B*, 2012, **116**, 5234–5241.
22 J. E. Glass, *J. Phys. Chem.*, 1968, **72**, 4450–4458.
23 G. Tesei, G. Paradossi and E. Chiessi, *J. Phys. Chem. B*, 2014, **118**, 6946–6955.
24 W. Thomson, *Proc. R. Soc. Edinburgh*, 1872, **7**, 63–68.
25 W. S. Ahn, M. S. Jhon, H. Pak and S. Chang, *J. Colloid Interface Sci.*, 1972, **38**, 605–608.
26 D. Brutin and V. Starov, *Chem. Soc. Rev.*, 2018, **47**, 558–585.
27 J. B. W. Webber, *Prog. Nucl. Magn. Reson. Spectrosc.*, 2010, **56**, 78–93.
28 W. A. Johnson, *Am. Inst. Min. Metal. Petro. Eng.*, 1939, **135**, 416–458.
29 M. Avrami, *J. Chem. Phys.*, 1939, **7**, 1103–1112.

